# Biot-Gassmann analysis of partial and patchy saturated reservoirs for both reflected and transmitted seismic waves

*James G. Berryman*

## ABSTRACT

This paper is a tutorial on the relationships between Biot-Gassmann theory for AVO-AVA analysis of reflection seismic amplitudes and also for the related analysis of propagation speeds for transmitted seismic waves in applications such as VSP or crosswell seismic. The main observation of special note is that the so-called "fluid-line" in AVO analysis appears to be related to patchy saturation of fluids when the Biot-Gassmann analysis of laboratory data is considered.

## INTRODUCTION

In this paper, I present a short analysis of and comparison between the well-known Amplitude Versus Offset (AVO) approach (**?????**) — as well as for Amplitude Versus Angle [for AVA, see **?** and **?**] — for identifying fluid content in reservoirs from seismic reflection data and the predictions of Gassmann's equations for AVO reflectivity analysis. In addition other distinct types of seismic wave analysis based on wave velocities alone will be considered in the same context (**???**). Some of these cases of most interest may not involve any reflections, only transmission of the waves through the reservoir of interest. In such cases, the wave speed/velocity analysis presented can in fact be used in the absence of reflectivity data, for example, in well-logging applications, VSP, or crosswell seismic tomography.

AVO analysis is a technique used to determine various physical properties of reservoirs, including density, porosity, bed thickness, velocity, and (most importantly) fluid content of rocks. This type of analysis tends to be more successful in young, poorly consolidated rocks, such as those in the Gulf of Mexico. Older, better consolidated, or well-cemented sediments from continental regions are not such good candidates for AVO studies.

One common failure of AVO comes from the inability to distinguish a gas-filled reservoir from one having only partial gas saturation (also known in this application as "fizz water"). As the Biot-Gassmann theory shows, shear wave energy of mode-converted waves at reservoir interfaces permits some levels of gas saturation to be distinguished. And one of the better ways of doing this is to use time-lapse analysis of seismic reflection data.

The analysis presented here will emphasize relations to the Biot-Gassmann theory (**???**) of fluid-saturated porous media. Although clearly important for explaining "bright spots" due to gas over oil, as well as many other issues in AVO, the Biot-Gassmann theory has seldom been treated carefully in this context due to the presence of so many other conflicting practical issues with the data analysis. I will nevertheless work through the predictions of Biot-Gassmann here, so our knowledge of this part of the science is clearly laid out for those who do find situations where it may be appropriate to take advantage of it. The Biot-Gassmann theory, when extended to the cases of partial and patchy saturation, can help to eliminate some of these ambiguities.

## AVO ANALYSIS AND ALTERNATIVES FOR SEISMIC REFLECTIONS

AVO analysis in isotropic layered systems uses the reflectivity moveout for compressional wave scattering (**??????**)

$$R(\theta) = A + B \sin^2 \theta, \tag{1}$$

where $R$ is the reflectivity, $\theta$ is the angle of incidence measured from the vertical so that $\theta = 0^o$ corresponds to vertical incidence, and $\theta = \pi/2$ $(= 90^o)$ is horizontal incidence. The coefficients $A$ and $B$ are called respectively the intercept and slope, because of their significance at $\theta = 0^o$ (for the intercept), and $\theta \neq 0^o$ (for the slope). Layering of physically distinct types of earth materials is implicitly required by this method, since the wave reflectivity vanishes if there is no contrast in the pertinent wave-related physical properties at such interfaces. Wave-related properties include: the elastic constants $K$ (bulk modulus) and $G$ (shear modulus), and also the inertial mass density $\rho$. A list of important physical properties could also include wave attenuation, but I will not discuss that issue in this paper.

Coefficients $A$ and $B$ depend on the elastic properties of the system through the wave speeds $v_p$ (compressional) and $v_s$ (shear) determined by the well-known relations

$$v_p^2 = (K + 4G/3)/\rho, \tag{2}$$

and

$$v_s^2 = G/\rho. \tag{3}$$

The bulk modulus and shear modulus are related to the Lamé elastic parameters $\lambda$ and $\mu$ for isotropic media (**??**) by $K = \lambda + 2\mu/3$ and $G = \mu$. For long-wavelength analysis, the density $\rho = M/\Omega$ includes all the mass $M$ (of solid, liquid, and/or gas) present in the volume $\Omega$.

Following **?** [but also see **?**, **?**, **?**, **?**, and **?**], we have equations for the reflectivity coefficients which are:

$$A = \frac{\Delta v_p}{2v_p} + \frac{\Delta \rho}{2\rho} = \frac{\Delta(v_p^2)}{4v_p^2} + \frac{\Delta \rho}{2\rho} \tag{4}$$

and

$$B = \frac{\Delta v_p}{2v_p} - 4\frac{v_s^2}{v_p^2}\left(\frac{\Delta v_s}{v_s} + \frac{\Delta\rho}{2\rho}\right) = \frac{\Delta(v_p^2)}{4v_p^2} - 2\frac{v_s^2}{v_p^2}\left[\frac{\Delta(v_s^2)}{v_s^2} + \frac{\Delta\rho}{\rho}\right]. \tag{5}$$

The meaning of the $\Delta$ in these formulas is clear, since I am referring to the differences in these quantities as the wave passes from one layer to the next. Thus, for example, $\Delta v_p$ is the change in the compressional wave speed $v_p$ across the interface. Since — for small changes (consistent with the analysis of Aki and Richards) — the reflectivities should be the same (except for the difference in sign due to the sign of the $\Delta$) whether the waves are up-going or down-going, it is clear that the quantities not differenced in these formulas must be averaged, *i.e.*, take half the sum of these quantities on each side of an interface. If these differences across the interfaces are very small, then the layer averaging step can be ignored altogether. Linearized parameter estimation techniques (**?**) are also consistent with these assumptions together with the additional caveat that reasonably good estimates of the background parameters must also be available from other means. The second version of each of these two formulas in (4) and (5) is presented to emphasize the fact that these quantities are really equivalent to logarithmic derivatives, and as such can be written in many different ways. The advantage of the second choice in each case is that, by squaring the velocities, we eliminate the square roots of the bulk and shear moduli, as well as those of the densities. These square roots would naturally fall away as we compute the relationships between coefficients $A$, $B$, and physical constants $K$, $\rho$, $G$. But it seems a bit easier to scan the math and, thereby, see where terms originate by introducing this intermediate step.

If the only change across the boundary of interest occurs in the nature — *i.e.*, the physical properties — of the pore fluid, then for isotropic materials I can take advantage of Gassmann's equations to note that the shear modulus $G$ does not depend on the fluid bulk modulus $K_f$, and, therefore, $G$ does not change under these circumstances within mixed-fluid-saturated reservoirs. Then, using the definitions of the wave speeds for isotropic elastic/poroelastic media, I have:

$$A = \frac{\Delta K}{4(K + 4G/3)} + \frac{\Delta\rho}{4\rho} \tag{6}$$

and

$$B = \frac{\Delta K}{4(K + 4G/3)} - \frac{\Delta\rho}{4\rho}. \tag{7}$$

By taking linear combinations of these two expressions, we can separate out the dependencies on the changes in bulk modulus $K$ and the density $\rho$, giving respectively

$$\frac{\Delta K}{2(K + 4G/3)} = A + B \tag{8}$$

and

$$\frac{\Delta\rho}{2\rho} = A - B. \tag{9}$$

Thus, these relations represent a very clean decoupling of the changes in the reflectivity coefficients *due to the fluid effects alone* (since, by present assumption, the fluid effects are the only variables present) in terms of the elastic and inertial physical parameters $K$ and $\rho$. And, at least for isotropic media, these are the two parameters that determine relationships between fluid properties and wave speeds.

## DENSITY AND BIOT-GASSMANN RELATIONS FOR THE BULK MODULUS

Of the two parameters $K$ and $\rho$, the easier physical parameter to analyze in the foregoing text is certainly the inertial density, which is given explicitly by

$$\rho = (1-\phi)\rho_s + \phi[S\rho_l + (1-S)\rho_g], \tag{10}$$

where $\phi$ is the porosity, $\rho_s$ is the solid density of the rock material (with no porosity), $\rho_l$ is the density of any liquid present (assuming only one such is present), and $\rho_g$ is the density of any gas present (again assuming only one such is present). The saturation $S = S_l$ refers to the liquid saturation, meaning that the parameter $0 \leq S_l \leq 1$ is a measure of the fraction of the pore space that is occupied by liquid. Then, the gas saturation is $S_g = 1 - S$, which is just the fraction of the pore space left to be occupied by the gas. This way of accounting for the density contribution assumes there are no dynamic effects of density in the seismic/acoustic/ultrasonic frequency domain of interest. For Biot theory (**??**), this assumption is an oversimplification, since there can be motion of the fluids, creating damping effects that make the inertial density effectively a complex number due to out-of-phase motion between the pore fluid and the surrounding solid matrix materials. I am typically assuming here that the frequencies of interest are those of field/seismic experiments, so they are usually less than about 20 kHz for well-logging, and more likely to be the range 10 to 100 Hz for reflection seismic work. Cross-well tomography can cover the frequencies between these two extremes. But all of these frequencies, up to about 1 kHz for sure (**?**), are low enough that the scalar constant density assumption made here is usually appropriate. The biggest concerns — if any — will come into play only at the very highest frequencies, and then for laboratory experiments, especially in the ultrasound range. (Laboratory data analyzed later is at higher frequencies, but — as is demonstrated — not so high as to invalidate the present discussion.)

Again, for low enough frequencies and isotropic solid matrix, it is normally adequate to treat the shear modulus as independent of both frequency and fluid-saturation. So we may assume that $G = \mu =$ constant [following the isotropic results of **?**]. But this assumption can also go wrong at high enough frequencies, or in the presence of anisotropic elastic behavior (Pride *et al.*, 2004; Berryman, 2005). We will ignore both of these effects in the following *simplified* analysis.

One alternative simplification of Equation (5) follows from this constancy of $G$ in

isotropic poroelasticity. In particular, I find that

$$\left[\frac{\Delta(v_s^2)}{v_s^2} + \frac{\Delta\rho}{\rho}\right] \equiv 0, \tag{11}$$

since $G$ is independent of the physical mechanisms that (I have assumed) are varying, so the $G$ dependence of this expression disappears, so that the remaining contribution is just:

$$\left[\frac{\Delta(\rho^{-1})}{\rho^{-1}} + \frac{\Delta\rho}{\rho}\right] = -\Delta\ln\rho + \Delta\ln\rho \equiv 0. \tag{12}$$

So it vanishes identically. Thus, for the Biot-Gassmann examples considered here, the slope $B$ is given simply by

$$B = \frac{\Delta(v_p^2)}{4v_p^2}. \tag{13}$$

Thus, only spatial variations in $v_p$ determine $B$, while variations in both $v_p$ and $\rho$ play roles in determining the value of $A = B + \Delta\rho/2\rho$ for this Biot-Gassmann analysis.

Another important observation based on the result (11) is the fact that the logarithmic derivative of the density can be replaced everywhere by the logarithmic derivative of $v_s^2$, using the relation:

$$\frac{\Delta\rho}{\rho} \equiv -\frac{\Delta(v_s^2)}{v_s^2}, \tag{14}$$

which is always true for the situations under consideration here. Thus, in these circumstances, I find that

$$A = \frac{\Delta(v_p^2)}{4v_p^2} - \frac{\Delta(v_s^2)}{2v_s^2}, \tag{15}$$

and

$$A - B = -\frac{\Delta(v_s^2)}{2v_s^2}. \tag{16}$$

## Seismic impedance analysis

Seismic impedance analysis (**?**) is based on ideas similar to those already presented, but the effort is concentrated now on the quantities $I_p \equiv \rho v_p$ and $I_s \equiv \rho v_s$, which are the seismic impedances that determine the values of the reflection and transmission coefficients for normal incidence at interfaces between layers. Clearly, we can reanalyze everything we have presented so far in terms of these impedances, since exactly the same physical quantites are involved: $\rho$, $v_p$, and $v_s$. To the order of approximation we are considering now, the coefficient $A$ is seen from (4) to be given by

$$A = \frac{\Delta I_p}{I_p}. \tag{17}$$

Then the intercept $A$ is just the logarithmic derivative of $I_p$ (which is basically how and why $I_p$ was defined in the first place). Obtaining a similar expression for the logarithmic derivative of $I_s$, requires consideration of similar measurements for the reflections of shear waves at boundaries. On the other hand, for the Biot-Gassmann analysis, I have $I_s = \sqrt{\rho G}$, with $G$ being constant across these boundaries, and therefore

$$\frac{\Delta I_s}{I_s} = \frac{\Delta \rho}{2\rho}, \tag{18}$$

so, from (9), I have

$$B = A - \frac{\Delta \rho}{2\rho} = \frac{\Delta I_p}{I_p} - \frac{\Delta I_s}{I_s}. \tag{19}$$

Thus, $B$ can also be interpreted as the difference in the two logarithmic derivatives of $I_p$ and $I_s$.

If direct measurements of these two impedances are available (perhaps from well-logs of density and wave speeds, for example), then other combinations of these quantities, may be considered and, in particular, I have $\rho\lambda = I_p^2 - 2I_s^2$ — where $\lambda = K - 2G/3$ is one Lamé constant. The advantage of studying the quantity $\rho\lambda$ is that this calculation has eliminated the part of the problem that is insensitive to fluids, namely the shear modulus $G$, which has disappeared altogether from this relationship. Thus, when various authors (**??**) compare plots of $v_p$, $I_p$, and $\rho\lambda$, it is typically found that the $\rho\lambda$ plots are the ones that are the most sensitive to fluid/liquid presence.

## Well-mixed gas-liquid mixtures: partial (liquid) saturation

Finally, I need to consider the bulk modulus $K$ for the fluid-filled system, and this modulus requires more discussion. First, for the isotropic case with a single fluid $F$, we have Gassmann's equation (**???**):

$$K_u = K_d + \frac{\alpha^2}{\frac{\alpha-\phi}{K_s} + \frac{\phi}{K_F}}, \tag{20}$$

where $K_s$ is the (assumed constant/uniform) bulk modulus of the solid material, $K_d$ is the drained modulus (for a porous system filled with air or other very compliant gas, this modulus is essentially the same as if all fluid is drained from the pores), $K_u$ is the undrained modulus (either the fluid is trapped by the boundary conditions, or the wave frequencies are so high that the system cannot relax significantly during one cycle), $\alpha = 1 - K_d/K_s$ is the **?** coefficient (also sometimes called the effective-stress coefficient), and finally $K_F$ is the bulk modulus of the assumed uniform fluid. The modulus $K_F$ can also be treated as the modulus of a uniformly mixed fluid, such as a liquid-liquid mixture, or a liquid-gas mixture. There is however an assumption of immiscibility implicit in the resulting formula for $K_F$, which — for liquid and gas

mixtures — is given by

$$\frac{1}{K_F} = \frac{S}{K_l} + \frac{1-S}{K_g}, \tag{21}$$

where $K_l$ is the bulk modulus of the liquid constituent, and $K_g$ is the bulk modulus of the gaseous constituent. As before, $S \equiv S_l$ is the liquid saturation level. Equation (21) is the volume weighted harmonic mean of the moduli of the two constituents [also known as the **?** average], and it is the exact result for quasi-static deformation of a well-mixed liquid-gas mixture.

Next, the most important fact to notice about (21) is that $K_g << K_l$ typically holds for liquids and gases. So, (21) implies that $K_F \simeq K_g/(1-S)$, unless $S \simeq 1$, in which case the formula reverts to the near equality $K_f \simeq K_l$. Thus, there is usually a broad range of values of saturation $S << 1$ for which $K_F$ behaves like $K_g$, and a narrow range of $S$'s, on the order of $0.95 \leq S \leq 1$, in which the liquid behavior becomes dominant. (See the discussion later on of Figure 1.)

## Patchy saturation

Now suppose that the fluids are not well-mixed, but actually very poorly mixed, so that each of the two fluids essentially occupies its own private compartments of the rock. Then, the correct formula for the undrained modulus is *not* given by (20). Instead we need to consider these two quite differently occupied compartments separately. Each compartment may still obey Gassmann's equation, but with $K_F = K_l$ in one compartment, and $K_F = K_g$ in the other compartment. So we have two distinct results, both valid simultaneously but for different spatial regions determined by the fluid $(g, l)$ saturant:

$$K_u^{(l)} \equiv K_d + \frac{\alpha^2}{\frac{\alpha-\phi}{K_s} + \frac{\phi}{K_l}}, \tag{22}$$

and

$$K_u^{(g)} \equiv K_d + \frac{\alpha^2}{\frac{\alpha-\phi}{K_s} + \frac{\phi}{K_g}}, \tag{23}$$

assuming that all the other properties except for the saturation levels are the same in the two compartments.

Next consider the observation that, since the shear modulus $G = \mu$ does not depend in any way on fluids (so $G_g = G_l = G$) if the porous material is locally isotropic, then we can take advantage of the rigorous and exact results for anisotropy due to layering. The known results on anisotropy due to layering by **?** and **?**, and later for the bulk modulus of general heterogeneous materials (when composed of isotropic materials) by **?** all produce the same general formula:

$$K_u^* = \left[ \sum_{f=g,l} \frac{S_f}{K_u^{(f)} + 4G/3} \right]^{-1} - 4G/3, \tag{24}$$

where the $*$ indicates the (overall) effective bulk modulus of the system as a whole, and again $S_g = 1 - S_l$. We should emphasize that the condition of constant shear modulus is not at all a trivial one, and it may not in fact be closely satisfied in many cases in practice. Furthermore, a more general pair of relations for bounds on overall bulk modulus is known, namely the Hashin-Shtrikman bounds **?**. These bounding relations of Hashin and Shtrikman have exactly the same functional form as (24), although with different choices for the shear modulus parameter $G$ (since $G$ is not unique in the heterogeneous system) — and also possibly the undrained bulk modulus parameters $K_u^{(f)}$ may differ as well — since these bounds are usually written for two-component media having $G = G_1$ or $G_2$. The logic of bringing in the Hashin-Shtrikman bounds into the discussion at this point is somewhat doubtful, however, since my main line of argument concerns a constant porous background medium with only variable fluid content. So I will not pursue this alternative point of view here. But it should be emphasized that use of these Hashin-Shtrikman bounds in the present context has considerable potential to produce misleading results, especially when the system has some local anisotropy present. [See **?** and **?**.] Nevertheless, if the local (when drained) porous medium is sufficiently isotropic and uniform, then these conditions, that are required for (24) to be valid, are then satisfied automatically. This somewhat limited result is then sufficient for the purposes of the present discussion.

Patchy saturation is clearly very pertinent to fluid distributions in the earth. It is also true that it must have frequently happened that laboratory data on partially saturated systems have been analyzed (in the absence of other, more detailed, information about fluid arrangement in the pore space) assuming that the spatial distribution of fluids did not matter, and then applying the Biot-Gassmann results for homogeneous saturation. One recent example of a recalculation for a system that was surely patchily saturated, but analyzed as if it were homogeneously saturated was the data of **?**, where he inappropriately analyzed his drainage data on porous cylinders using the Biot-Gassmann theory for homogeneous partial saturation. The observed results did in fact seemingly agree quite well with the theory in this case. But more recently **?** have reanalyzed Murphy's data assuming instead that the drainage process created a dry annulus surrounding a fully wet core in the porous cylinder. This fluid distribution would be consistent with a drying process that starts at the outside cylinder surface, and gradually works its way into the center of the cylinder. **?** show that the new analysis of these data actually agrees significantly better with the laboratory data than did the original homogeneous analysis of these same data by **?**. The patchy analysis is more difficult technically than was the earlier analysis, and that is one reason that it took more than 20 years for this reanalysis to appear.

## Saturation proxy

If the inertial density of the partially or patchily saturated medium is given by $\rho = (1-\phi)\rho_s + \phi(S_l\rho_l + S_g\rho_g)$, where again $S_g = 1 - S_l = 1 - S$, then the inverse of the

shear velocity squared can be used as a liquid saturation proxy via:

$$S_{proxy} \equiv \frac{(1/V_s^2)|_S - (1/V_s^2)|_{S=0}}{(1/V_s^2)|_{S=1} - (1/V_s^2)|_{S=0}} = \frac{\rho|_S/G - \rho|_{S=0}/G}{\rho|_{S=1}/G - \rho|_{S=0}/G} = \frac{\rho|_S - \rho|_{S=0}}{\rho|_{S=1} - \rho|_{S=0}} = S_l. \tag{25}$$

The point of showing the various steps in (25) is that, since the shear modulus $G$ is independent of the fluids within isotropic poroelastic media [but see **?** and **?**], $G$ cancels out in the next to last step — thus producing the desired result. This approach requires the auxiliary data $V_s|_{S=0}$ and $V_s|_{S=1}$, which can presumably be estimated either from data in other differently saturated spatial locations in the same reservoir, or from time-lapse data at the same location in the reservoir, as the liquid saturation level declines or increases. This fact can be useful (**?**) when saturation data are not available, but will not be considered further here.

## EXAMPLES AND DISCUSSION

AVO analysis typically concentrates on observations of the so-called "fluid line," which on a plot of $B$ versus $A$ is the line defined by $B = -A$, from the upper left through the origin at $(A, B) = (0, 0)$ down to the lower right. The nominal "hydrocarbon line" is the vertical line for all $B$ values at fixed $A = 0$, and other points in a vertical band in the close vicinity of this line.

These "rules" are typically gleaned from field experience, rather than from tight connections to the physical principles embodied in the Biot-Gassmann theory of porous media containing fluids. Part of the problem regarding the physics versus the field experience is lack of sufficient knowledge – both of the porous earth medium in situ, and also of the various pertinent details of the properties and spatial arrangement of the fluids themselves. So it is not unusual to see discussions of these AVO methods without any reference at all to the Biot-Gassmann literature for seismic waves in fluid-saturated or partially (possibly patchily) saturated porous media.

Figures 1-9 all make use of laboratory data by **?** on Spirit River sandstone. This sandstone has porosity $\phi = 0.052$, and fluid permeability of $1\mu$D. Measurements were made with piezoelectric transducers having resonant frequencies of 1 MHz for the $v_p$ measurements, and 600 kHz for the $v_s$ measurements. (These frequencies are high compared to the earlier discussion, but the data displayed indicate the prior analysis is valid nevertheless.) Maximum saturation attained was $S_w = S_l = 0.9$. We can think of these results as time-lapse data with imbibition carrying the liquid saturation from zero to 0.9, and with drainage carrying the saturation from 0.9 back to zero. Clearly a type of hysteresis is observed in these data, as the curves do not lie on top of each other. Rather, what is seen is surely (based on interpretations of the Biot-Gassmann theory for homogeneous and patchy saturation) homogeneous saturation along the imbibition curve, and patchy saturation along the the drainage curve (**?**). For $S_w = S_l <\simeq 0.3$, the two curves essentially coincide. The precise location of this coincidence point is hard to predict as it must depend in detail on the

connectedness of the pore space, and so is typically not known unless other methods such as x-ray imaging have been implemented to determine this normally missing information.

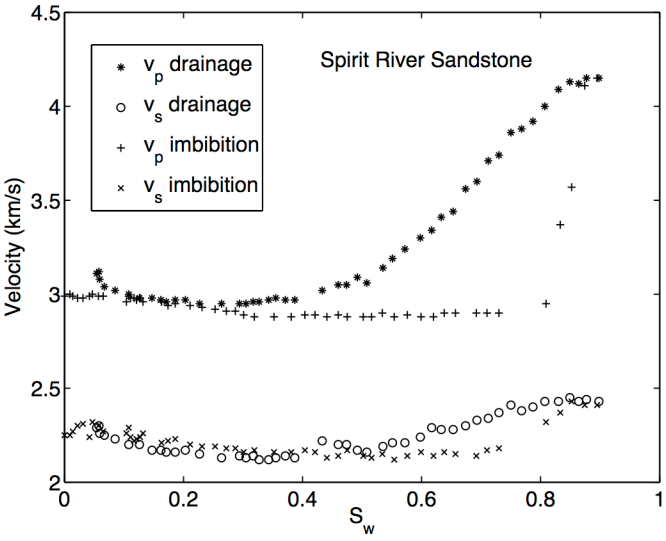


Figure 1: Spirit River sandstone data of **?** for both drainage and imbibition methods of changing the liquid saturation levels. Note that imbibition is a time-lapse experiment with $S_w$ increasing from zero to its maximum value. Similarly, draingage is a time-lapse experiment with $S_w$ decreasing from its maximum value to zero. Thus, the compressional wave data show explicitly effects due to the fact that the fluid saturation is patchy for drainage, but nearly homogeneous for imbibition. [**NR**]

Color is used in Figures 2 through 9 to highlight those parts of the two data sets where the most rapid changes are occurring in $v_p$. For Figures 2-5, these values are from approximately $S_w = 0.8$ up to $S_w = 0.9$, and the points are shown in blue. For Figures 6-9, these values are from approximately $S_w = 0.4$ up to $S_w = 0.9$, and these points are shown in red.

Previously mentioned observations from AVO analysis tend to emphasize that the so-called "fluid line" ($B = -A$) and the hydrocarbon line ($A = 0$) are actually *not* prominent in the observed behavior in Figures 2-5 for homogeneous saturation. Thus, these imbibition data do not seem to show the usual behavior associated with AVO plots of field data. This fact may indicate instead that field data typically display heterogeneous — or patchy saturation — characteristics.

In Figures 6-9, important differences from Figures 2-5 are observed, including the fact that, whereas the homogeneous saturation results for Figure 2-5 do not display the anticipated results for data lying along the so-called "fluid line" at $B = -A$, it is nevertheless easy to see that the patchy saturation data (*i.e.*, the red data points in Figures 6-9 for $S_w = 0.4$ up to $S_w = 0.9$) clearly do fall along this $B = -A$ line in Figure 6, for these Spirit River Sandstone ultrasonic data. This observation suggests that the empirically observed "fluid line" may actually be a mixed or patchy saturation line — since viscous hydrocarbons and different densities of both oil and gas are commonly found in situ. Since hydrocarbons were not used as the fluids in these laboratory exepriments, I cannot say more about the lack of any hydrocarbon line (*i.e.*, $A = 0$) behavior in either of these data plots.

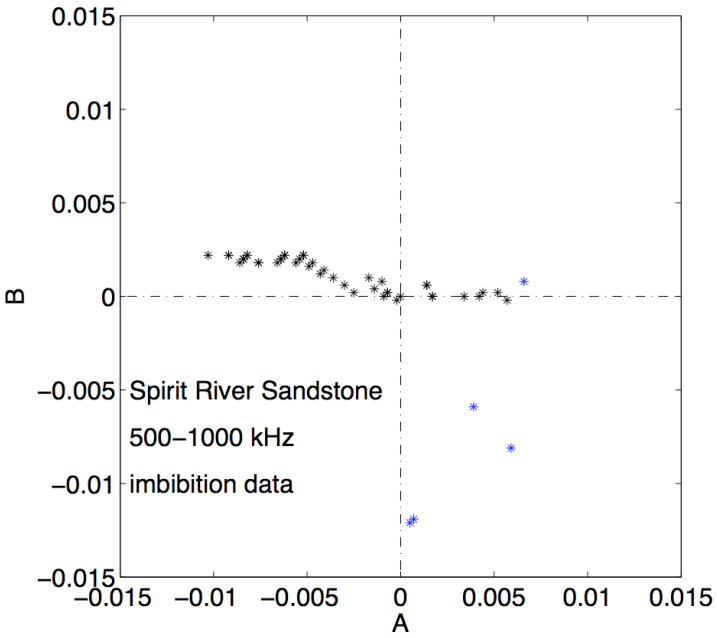


Figure 2: The next four figures show a comparison of four ways to view wave speed data and/or wave speed change data (via measured reflection coefficients). Laboratory data of **?** on Spirit Rive sandstone is used as the example, because both imbibition (quasi-homogeneous saturation) and drainage (patchy saturation) examples are available. Figure 2 show the usual display for AVO data of intercept $A$ versus slope $B$. [**NR**]

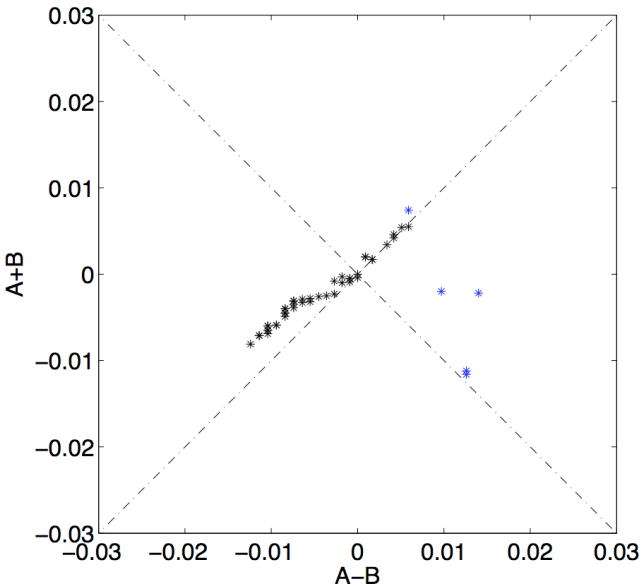


Figure 3: This figure shows how these same data from Figure 1 may be displayed by taking different combinations, namely $A - B$ and $A + B$. This approach is basically a rotation of the usual display in Figure 2, but the boundaries also expand by a factor of two. [**NR**]

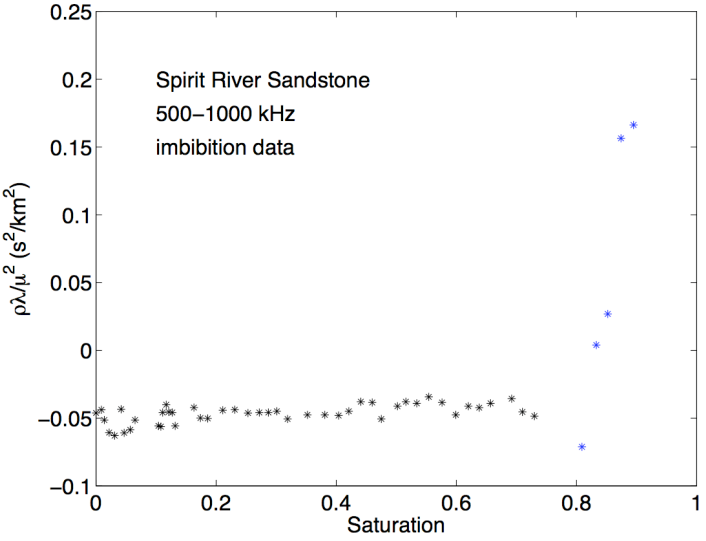


Figure 4: This third display of the imbibition data emphasizes $\rho\lambda = I_p^2 - 2I_s^2$ versus saturation, although it is actually $\rho\lambda/\mu^2$ that can be computed most easily from available velocity data. This is a display that could also be obtained using well-log data $(\rho, v_p, v_s)$. [**NR**]

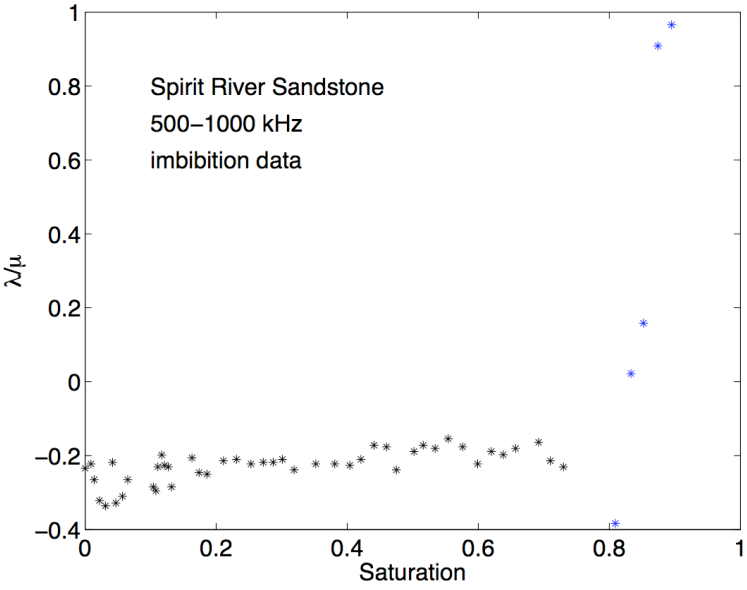


Figure 5: This fourth and last display of the imbibition data is very similar to Figure 4, but does not require independent information about the density $\rho$, so it is also pertinent to both VSP and cross-well seismic data. Note that in Figures 2-5, these imbibition data do not seem to show the usual behavior associated with AVO plots of field data, which may indicate that the patchy saturation model is the more appropriate one to use when analyzing field data. [**NR**]

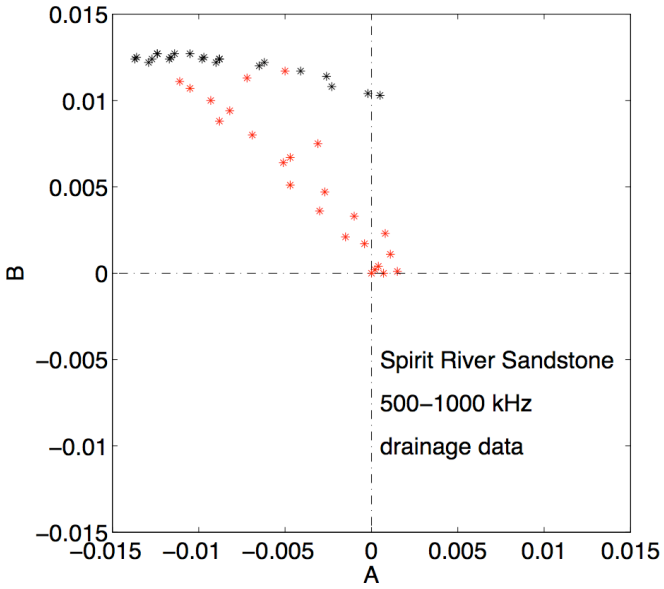


Figure 6: Like Figure 2, but for drainage data and therefore patchy saturation. Note that the most interesting parts of the data set (having more liquid present) do in fact fall along the $B = -A$ "fluid-line" in this Figure, as is also often seen empirically in field data. [**NR**]

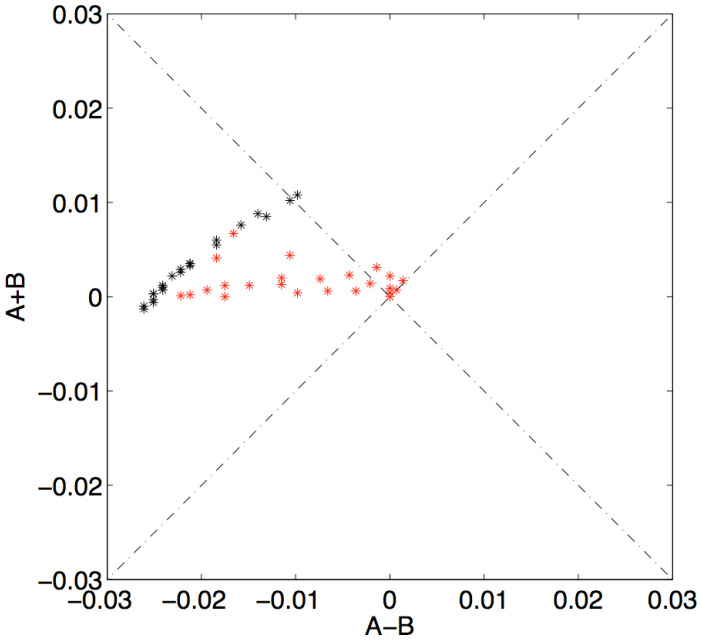


Figure 7: Like Figure 3, but for drainage data and patchy saturation. [**NR**]

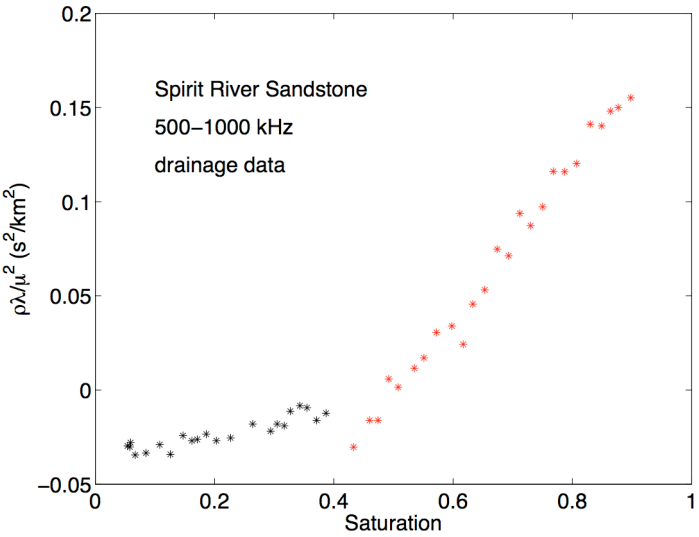


Figure 8: Like Figure 4, but for drainage data and patchy saturation. [**NR**]

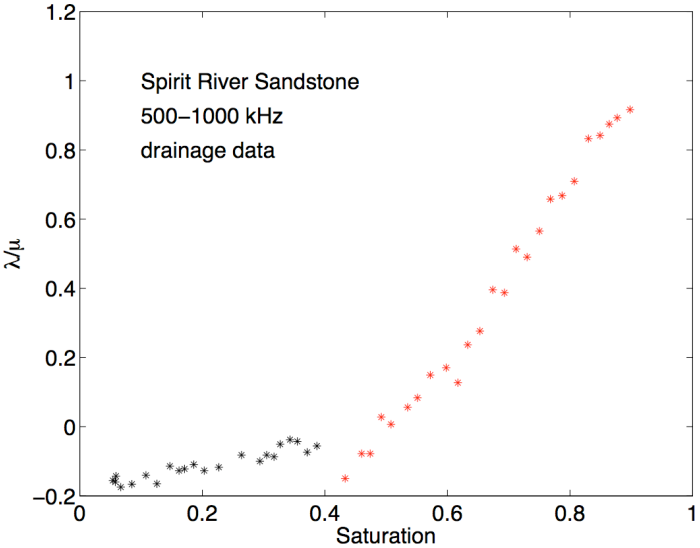


Figure 9: Like Figure 5, but for drainage data and patchy saturation. Again note how similar Figures 8 and 9 are, showing that most of the useful information is in $\lambda$, not $\rho$. [**NR**]

## ACKNOWLEDGMENTS

I would like to thank Steven R. Pride for helpful comments and references.

## REFERENCES